Journal of Fluorescence, Vol. 14, No. 4, July 2004 (©2004)

Label Free Colorimetric Biosensing Using Nanoparticles

Nidhi Nath[1,2] and Ashutosh Chilkoti[1,3]

Received December 15, 2003; revised February 3, 2004; accepted February 3, 2004

In this review article, we discuss a class of biosensors that exploit the change in the colorimetric properties of noble metal nanoparticles in response to biomolecular binding at their surface. Several sensor fabrication techniques as well as sensor configurations are discussed with an emphasis on their strengths and limitations. We conclude by presenting the future prospects and challenges for the successful transition of this technology from the laboratory to a commercial product.

KEY WORDS: Gold and silver nanoparticles; surface plasmon resonance; self assembled monolayer; protein-ligand binding; biosensor.

INTRODUCTION

The direct, label-free transduction of biomolecular interactions into a physico-chemical signal that can be easily and sensitively quantified in real-time is critical to applications in clinical diagnostics, real-time detection of environmental and biological toxins for field-use, and in proteomics. Various approaches to exploit advances in nanoscience and nanotechnology for bioanalysis have been recently reported, as the thrust in biosensor research moves towards miniaturization and multiplexing so as to simultaneously and rapidly detect a large number of analytes in ever-smaller volumes to increase sensitivity and throughput and reduce cost.

The direct transduction of biomolecular binding has been recently demonstrated by a wide range of nanoscale transduction mechanisms. Nanometer scale bending of microfabricated cantilevers in response to biomolecular binding [1] has been used to detect clinically relevant concentrations of prostate-specific antigen [2]. The reorientation of liquid crystals tethered to a nanostructured gold surface in the presence of low molecular weight organic molecules (e.g. organophosphorous or organoamine) has been shown to trigger a visual change that can be used to sense these chemical agents at parts-per-billion concentration in the atmosphere [3]. The fabrication of protein nanoarrays using dip-pen-nanolithography and their use for the detection of protein binding by measuring the change in the height of the nanoarray by AFM has also been recently reported [4].

In a quest for technologies that meet the demands of bioanalytical detection—real time detection, high sensitivity, high throughput, and low sample volume—several groups including ours are investigating the use of noble metal nanoparticles and nanostructures[4] as optical transducers of biomolecular binding events. The optical transduction by noble metal nanoparticles is based upon the phenomenon of nanoparticle surface plasmon resonance (nanoSPR). NanoSPR is the collective oscillations of surface electrons induced by visible light and is responsible for the intense colors exhibited by colloidal solutions of noble metals such as gold and silver. NanoSPR is an interfacial phenomenon, and can be used in two complementary colorimetric modes to transduce biomolecular binding events at the nanoparticle surface. In the first—interparticle—mode, changes in the proximity of gold or silver nanoparticles due to their aggregation in suspension causes a large change in the extinction spectrum of

[1] Department of Biomedical Engineering, Duke University, Durham, North Carolina.

[2] Current address: Promega Corporation, 2800 Woods Hollow Road, Madison, Wisconsin.

[3] To whom correspondence should be addressed. E-mail: chilkoti@acpub.duke.edu

[4] Nanoparticles refers to particles prepared by wet chemical synthesis whereas nanostructures refers to nanoparticles that are directly fabricated by lithography on a substrate.

1053-0509/04/0700-0377/0

the nanoparticle suspension due to long-range coupling of surface plasmons. The interparticle distance-dependent color change of silver or gold nanoparticles due to their aggregation has been used in solution-based immunoassays [5], and has been used by Mirkin and colleagues to design DNA sensors with femtomolar sensitivity [6–8]. In the second—intraparticle mode, the optical signal arises from the dependence of the peak intensity and position of the surface plasmon absorbance of gold and silver nanoparticles upon the local refractive index of the surrounding medium, which is altered due to binding at the nanoparticle-solution interface [9,10]. In this review, we focus on this latter mode of optical transduction of biomolecular binding at the interface of the nanoparticle-solution interface.

NOBLE METAL BIOSENSORS: THEORY

Noble metal nanoparticles (e.g., gold and silver) display unique size, shape and composition dependent optical properties. For example, an aqueous solution of gold and silver particles of 20 nm diameter appears brilliant red and yellow respectively. Gold and silver belong to a family of "free" electron metals that have a filled valence shell but an unfilled conduction band. The colors exhibited by nanoparticles of these metals arise through interaction of incident light with the "free" electrons resulting in resonant excitation of an oscillating dipole [11,12].

Mie first proposed a theoretical model to explain the optical extinction (sum of the absorption and scattering properties) of spherical noble metal nanoparticles. The optical extinction of nanoparticles with a radius (r) that is much smaller than the wavelength of light ($2r \ll \lambda$) can be adequately explained by the simplified Mie formula (Eq. 1) [13,14].

$$\sigma_{\text{ext}}(\omega) = 9\frac{\omega}{c}\varepsilon_{\text{m}}^{3/2}VN\frac{\varepsilon_2(\omega)}{[\varepsilon_1(\omega)+2\varepsilon_{\text{m}}]^2+\varepsilon_2(\omega)^2} \qquad (1)$$

where σ_{ext} is the extinction coefficient of the nanoparticles and is the sum of the absorption and scattering contributions, $\omega(=2\pi\nu)$ is the angular frequency of the incident light, $\varepsilon_{\text{m}}(=n_{\text{med}}^2)$ is the wavelength independent dielectric constant of the medium surrounding the nanoparticles, $\varepsilon(\omega)=\varepsilon_1(\omega)+i\varepsilon_2(\omega)$ is the wavelength dependent dielectric constant of the metal nanoparticles, and is assumed to be the same as that of the bulk material. $\varepsilon_1(\omega)=n^2-k^2$ and $\varepsilon_2(\omega)=2nk$, where n is the refractive index and k is the extinction constant of bulk gold or silver. $V(=4/3\pi r^3)$ is the nanoparticle volume and N is the number density of the nanoparticles.

According to Mie theory, the resonance condition is dependent on the refractive index of the medium and is fulfilled at a wavelength when

$$\varepsilon_1(\omega) = -2\varepsilon_{\text{m}} \qquad (2)$$

At resonance, nanoparticles display a maximum in their optical extinction. In intraparticle nanoSPR, binding of a target biomolecule to a receptor-functionalized nanoparticle in aqueous solution increases the local refractive index (i.e. increases the value of ε_{m}) of the surrounding medium. Because the dielectric constant ($\varepsilon_1(\omega)$) of gold and silver decreases with increasing wavelength [15], Eq. (1) shows that an increase in ε_{m} redshifts the resonance wavelength as well as increases the extinction at resonance—a property that forms the basis of optical transduction of receptor-analyte binding in intraparticle nanoSPR.

In interparticle nanoSPR, which is caused by aggregation of nanoparticles, a redshift is observed in the plasmon resonance accompanied by an increase in the extinction at higher wavelengths (>600 nm) and a broadening of the extinction band. The changes in the optical properties of the aggregates are caused by the change in the electromagnetic (EM) field strength experienced by the nanoparticles. The effective EM field strength experienced by an individual nanoparticle in an aggregate, is the combination of the incident electric field and the scattered EM field from neighboring particles. The optical properties of the aggregate depend on several parameters [13,16], which include the number of nanoparticles in an aggregate, the shape of the nanoparticles, the distance between particles in the aggregate, and the volume fraction and orientation of the aggregate with respect to polarized light.

BIOSENSING USING NOBLE METAL NANOPARTICLES[5] SYNTHESIZED FROM WET CHEMICAL SYNTHESIS

In this section we discuss the use of chemically synthesized noble metal nanoparticles in two alternative formats for the development of intraparticle nanoSPR biosensors: (1) solution based nanoSPR sensors and (2) surface nanoSPR sensors. Both of these modalities rely upon the availability of chemically synthesized nanoparticles, and we therefore first briefly summarize the current state of the art in the chemical synthesis of different types of nanoparticles that can be used to fabricate nanoSPR biosensors. Next, we review the use of these nanoparticles as optical transducers for solution-based sensors, followed by a discussion of a sensor in chip format, which involves the

[5]Spherical nanoparticles are referred to by the generic name of nanoparticles but anisotropic particles are referred by their specific shape (e.g. nanoprisms, nanorods, nanoshells, nanocubes).

immobilization of these nanoparticles on optically transparent substrates.

Wet Chemical Synthesis

A typical synthesis of spherical nanoparticles of gold or silver involves reduction of its metal salt in solution, and proceeds in three stages [17–19]. In the first stage, metal ions are reduced to metal atoms, which then undergo rapid collisions to form stable icosahedral nuclei of 1–2 nm in size. The initial concentration of nuclei depends on the concentration of the reducing agent, the solvent, temperature and reduction potential of the reaction. This stage, which is typically complete in a few seconds, is important because it determines the heterogeneity in the size and shape of the nanoparticles. Further growth of the nanoparticles occurs, in the second stage, by reduction of metal ions on the surface of the nuclei, until all the metal ions are consumed. The third and final stage involves prevention of nanoparticle aggregation, which is typically achieved by the addition of stabilizing agents. For example, gold nanoparticles are stabilized by electrostatic repulsion due to adsorbed citrate ions on their surface that impart negative charge to the nanoparticles. Gold nanoparticles with diameters in the range of 2–5 nm have been stabilized by thiol-capping agents [20]. Poly(vinylpyrollidone) (PVP) and bis(p-sulfonatophenyl)-phenylphosphine (BSPP) have been used to stabilize silver nanoparticles [21,22]. Adsorbed proteins can also stabilize nanoparticles, and prevent their aggregation at high salt concentrations.

The size of nanoparticles is controlled by varying the ratio of the reducing agent to metal salt. Increasing the molar ratio of reductant to metal salt causes rapid formation of a large number of nuclei and leads to smaller, monodisperse metal nanoparticles. In contrast, decreasing the molar ratio leads to slow formation of a few nuclei, and results in larger nanoparticles with a greater heterogeneity in size. Figure 1 shows the inverse dependence of the size of gold nanoparticles, on the molar ratio of sodium citrate to hydrogen tetrachloroaurate. Another method to control the size of metal nanoparticles is by using different combinations of reductant and stabilizing agent. For gold nanoparticles, the use of sodium citrate as the reductant results in spherical nanoparticles with a diameter in the range of 12–100 nm, whereas the use of white phosphorus produces nanoparticles with a diameter of 5–12 nm [23]. Even smaller particles of few nanometers in diameter can be synthesized by reduction of $HAuCl_4$ in an organic solvent in the presence of a thiol-capping agent [20]. For silver nanoparticles, the reduction of silver nitrate by

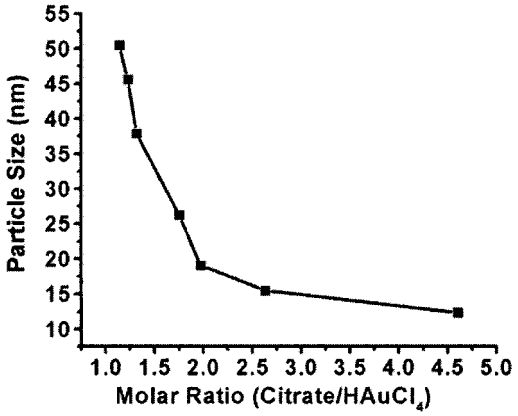

Fig. 1. The size of gold nanoparticles as a function of the molar ratio of sodium citrate to hydrogen tetrachloroaurate ($HAuCl_4$).

sodium borohydride in the presence of BSPP [22] results in the formation of ∼8 nm diameter particles whereas the use of PVP as the reducing and protective agent results in larger particles with diameters that range from 15 to 36 nm [21].

Due to their unique shape-dependent optical properties, substantial efforts have been devoted to the synthesis of anisotropic particles such as high-aspect ratio nanorods [24], multimetal micrometer rods [25], silver nanoprisms [26], and silver and gold nanocubes [27]. The different growth rates of various faces of the nuclei can be exploited to synthesize anisotropic nanostructures. In one synthetic approach, nanoparticles are physically entrapped inside rod-like micelles or nanotubes so as to force their growth in a specific crystallographic direction, leading to the formation of high-aspect ratio nanorods and nanowires [24,28,29]. Polymers can also reduce or enhance the growth of nanoparticles in a specific crystallographic direction resulting in the formation of structurally anisotropic nanoparticles. For example, PVP is believed to reduce growth rate in the ⟨100⟩ directions and/or increase growth rate in the ⟨111⟩ direction, to produce nanocubes [27]. Inhomogeneous core-shell nanoparticles are of interest for biosensing, because their optical properties can be independently controlled by changing the thickness of the shell and by the overall diameter of the core-shell nanoparticle (Fig. 2). Core-shell nanoparticles can be chemically synthesized by a number of routes such as silica nanotemplate-assisted electroless deposition [30] or by using silver nanoparticles as sacrificial templates [31].

These chemical strategies for the control of the size and shape of gold and silver nanoparticles are extremely valuable because the optical properties of these nanoparticles are dependent on their size and shape. The

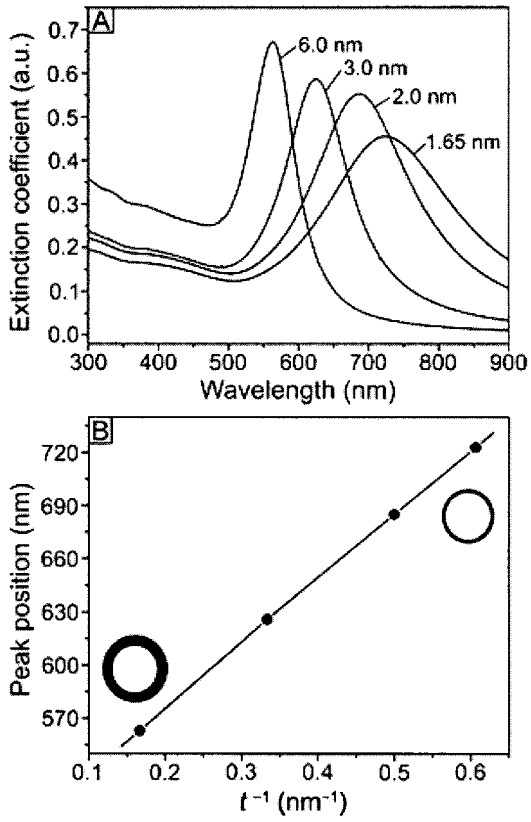

Fig. 2. (A) Calculated extinction spectra of spherical gold nanoshells with a core diameter of 25 nm and a shell thickness of: 1.65, 2.0, 3.0, and 6.0 nm. (B) The relationship between the peak extinction wavelength (peak position, nm)) and the reciprocal of shell thickness (t^{-1}, nm^{-1}): max $= 503 + 363t^{-1}$. Reprinted with permission from *Analyst* 2003, **128**, 686–691. Copyright 2003 Royal Society of Chemistry.

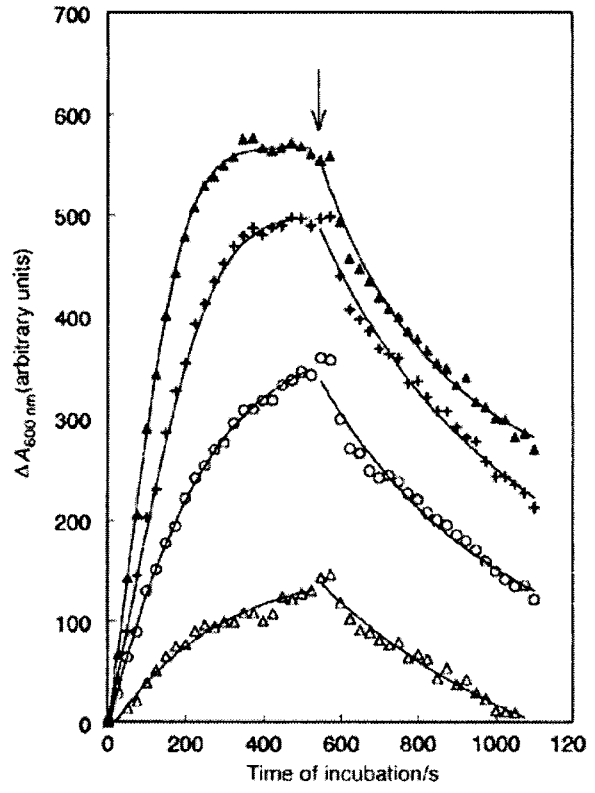

Fig. 3. Association and dissociation kinetics for binding of an anti-human heart fatty acid binding protein (hFABP) to gold nanoparticles coated with an anti hFABP antibody. The change in extinction at 600 nm was measured in a commercial clinical analyzer. The hFABP dose added to 180 μL solution of gold nanoparticles were 0.5 ng (Δ), 0.9 ng (○), 1.9 ng (+), 3.3 ng (▲). Reprinted with permission from *Analyst* 1998, **123**, 1599–1603. Copyright 1998 Royal Society of Chemistry.

optical properties, in turn, control the performance of these nanoparticles as optical transducers in nanoSPR sensors.

Solution-Based NanoSPR Sensor

The different types of gold and silver nanoparticles described previously can be used as optical transducers for nanoSPR. The refractive index-dependent color change of spherical, homogeneous gold nanoparticles was first used to develop a solution phase immunoassay to monitor the binding kinetics of antibody-antigen interactions in real time [32,33]. In these seminal studies, 40 nm gold nanoparticles, synthesized by citrate reduction of a hydrogen tetrachloroaurate solution, were coated with monoclonal antibodies specific for human ferritin, human chorionic gonadotropin (hCG) and human heart fatty acid binding protein (hFABP). Incubation of the antibody-coated nanoparticles with a solution of their antigen caused a red shift in the SPR extinction as well as an increase in the extinction at 600 nm. The increase in the extinction at 600 nm was used to track the dose dependent antibody-antigen binding kinetics (Fig. 3) and quantify the affinity of the interaction. The assay was performed in an automated clinical analyzer, which also demonstrated the feasibility of high-sample throughput. These studies were important because they set the stage for the use of gold and silver nanoparticles for clinical diagnostics and sensing.

Chip-Based NanoSPR Sensor

Overview

In this section, we review recent progress in the fabrication and characterization of chip-based nanoSPR sensors. Chip based nanoSPR biosensors, in which nanoparticles are immobilized on an optically transparent substrate, are attractive because the sensor chips can be fabricated and interrogated in an array format for rapid,

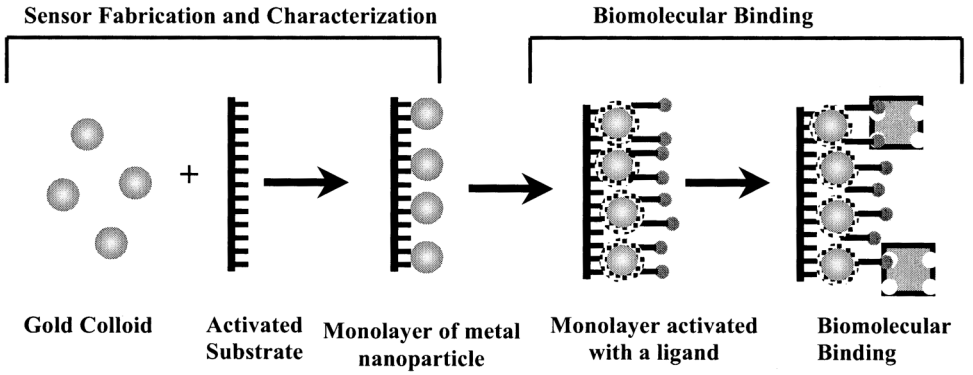

Fig. 4. The steps involved in the fabrication of a nanoSPR biosensor and its use for quantification of biomolecular interactions.

high-throughput screening of biomolecular interactions. In this review of chip-based nanoSPR architectures, we discuss the two components that together constitute a surface-based nanoparticle SPR biosensor—the optical transducer and biological detector. We emphasize in this discussion the characterization the sensing volume and sensitivity of the sensor to the changes in the local refractive index. We then describe coupling of the biomolecular detector to the optical transducer to create a functional nanoSPR sensor, which involves: (a) activation of the nanoparticle surface and immobilization of the receptor and (b) binding of target biomolecules and characterization of the sensor performance (Fig. 4).

The development of chip-based nanoSPR sensors was stimulated by the studies of Natan and colleagues who showed that gold nanoparticles can be self-assembled from solution onto a glass surface that was functionalized with amine or thiol groups [34,35]. The assembly of anionic, citrate stabilized gold nanoparticles on these functionalized surfaces is controlled by strong attractive interactions between the nanoparticles and the functional groups on the surface and by repulsive electrostatic interactions between the gold nanoparticles. This approach of chip fabrication is technically simple, yields reproducible and stable immobilized gold nanoparticles on glass, and can be easily scaled up for manufacturing. An added advantage of solution-based assembly of chemically synthesized nanoparticles is the ability to control the nanoparticle density on the surface by changing the solution conditions during colloidal self-assembly. A significant limitation of this method, however, is that nanoparticle assembly on the surface occurs via spatially random adsorption without long-range order so that fabrication of a periodic array of nanostructures on the surface is not possible by this method.

Okamoto and colleagues first demonstrated that gold nanoparticles, self-assembled on a functionalized glass surface optically respond to a change in the local refractive index induced by spin casting polymers of different thickness onto the immobilized gold nanoparticles [36]. They showed that both the resonance wavelength as well as peak absorbance of the immobilized nanoparticles increased with an increase in thickness of the spincast polymer film. We have further extended this concept by demonstrating proof-of-principle of a colorimetric biosensor in a chip format that is capable of real-time, label-free detection of biomolecular binding [9]. We showed that the change in refractive index caused by receptor-ligand binding at the surface of the nanoparticle causes a large enough optical change that enables real-time monitoring of the kinetics of binding of a model receptor and analyte.

Fabrication and Optical Characterization of a NanoSPR Chip

The major steps in the fabrication of a functional nanoSPR sensor are: fabrication and characterization of the nanoparticle optical transducer, characterization of the receptor ligand binding system that acts as a biological detector and coupling of the optical transducer to the biological detector to create a functional nanoSPR sensor (Fig. 4). The fabrication of the optical transducer involves activation of a glass substrate (or other optically transparent material) and self-assembly of metal nanoparticles on the functionalized glass substrate. A variety of different "receptors" such as antibodies and their engineered fragments, DNA and peptide nucleic acid aptamers, peptides and synthetic receptors of non-biological origin are available or are under development for different analytes of interest [37–39], and are not discussed further in this article. The final step in the fabrication of the sensor is activation of the nanoparticle surface and coupling of the receptor to the transducer. We discuss each of these steps in greater detail in the remainder of this section.

The first step in the self-assembly of nanoparticles on the glass surface is to introduce amine or thiol groups to enable chemisorption of the metal nanoparticles to the surface [34]. The preferred route for introduction of these moieties is by silanization of the glass surface using amine- or thiol-terminated alkoxysilanes [40]. Two forces drive the assembly of gold nanoparticles on an amine-functionalized surface: diffusion of negatively charged nanoparticles towards the positively charged amine-functionalized surface and interparticle repulsion between the negatively charged nanoparticles on the surface. The solution concentration of nanoparticles, time of incubation, temperature, pH and ionic strength of the solution are variables that can be used to control the density of the chemisorbed nanoparticles on the surface. Negatively charged nanoparticles can also be assembled on the surfaces coated with positively charged polymers such as polylysine and polyethyleneimine. The assembly needs to be stable in water, so that the assembled nanoparticles remain stably bound to the surface upon extended incubation in an aqueous solution, conditions that are commonly encountered in most biosensors. It is also important that the surface immobilization of the nanoparticles does not interfere with their subsequent functionalization to enable presentation of the receptor at the nanoparticle-solution interface.

The sensitivity of immobilized nanoparticles to the change in refractive index of the surrounding environment can be easily determined experimentally. Monolayers of nanoparticles are prepared on glass and immersed in different solvents with refractive indices ranging from 1.33 to 1.495 and their extinction spectra are measured in the range of 350–850 nm. An illustrative example (Fig. 5A) shows a red shift in the peak resonance wavelength as well as an increase in the peak extinction as a function of the solution refractive index. The shift in peak resonance wavelength ($\Delta\lambda^{max}$) is 72 nm/RIU (RIU = refractive index unit) and the change in maximum extinction (ΔExt^{max}) as well as the change in extinction at 575 nm ($\Delta Ext_{575\,nm}$) is linear as a function of refractive index (Fig. 5B). The measurement at an off-peak resonance wavelength of 575 nm was chosen for subsequent studies because it is experimentally easier to implement.

We also investigated the influence of particle size on the sensitivity of nanoSPR sensor by fabricating sensor chips with seven different sizes of gold nanoparticles with diameters ranging from 12 to 50 nm. The shift in peak resonance wavelength ($\Delta\lambda^{max}$) as a function of the refractive index of the solution is relatively constant with nanoparticle size. However the extinction sensitivity, defined as $\Delta Ext_{575\,nm}$/RIU, increases from 0.4 for 12 nm diameter gold particles to 1.25 for ~40 nm diameter particles.

Previous studies have shown that, for anisotropic particles, the shift in the resonance wavelength is more sensitive to the local refractive index when compared to spherical nanoparticles [41]. Preliminary experiments in our laboratory using spherical silver nanoparticles and silver prisms corroborate this finding. The wavelength sensitivity, defined as $\Delta\lambda^{max}$/RIU, of 120 nm and 220 nm for the spherical nanoparticles and prisms were obtained. A similar study by Xia *et al.* using hollow gold nanoshells assembled on glass showed a much larger $\Delta\lambda^{max}$/RIU of 408.8 [42]. These observations are also consistent with the theoretical work by Schatz and colleagues, who showed that anisotropic nanoparticles have a much higher EM field enhancement due to plasmon resonance as compared to spherical particles [43,44]. Together these studies demonstrate that the optical response of metal nanostructures to changes in the local refractive index is a complex function of their composition, size and shape. Recent advances in solution based synthesis of anisotropic nanoparticles, such as shells, prisms, rods and cubes, now provide an

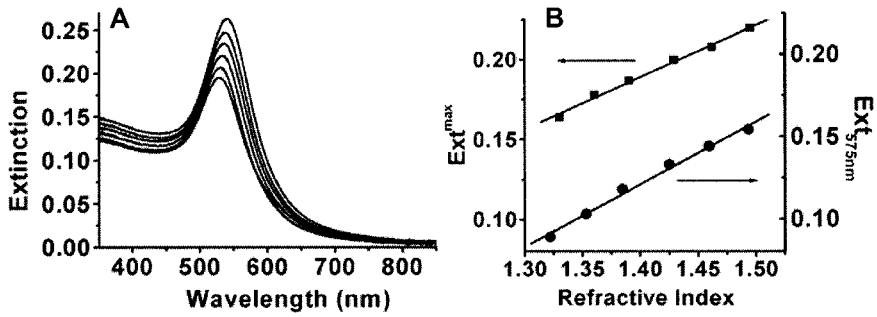

Fig. 5. Extinction spectra and plot of Ext^{max} and $Ext_{575\,nm}$ as a function of the refractive index of the surrounding medium for 12 nm diameter gold particles. The solvents were: water ($n = 1.33$), ethanol ($n = 1.36$); 3:1 (v/v) ethanol:toluene ($n = 1.39$), 1:1 (v/v) ethanol:toluene ($n = 1.429$), 1:3 (v/v) ethanol:toluene ($n = 1.462$), and toluene ($n = 1.495$).

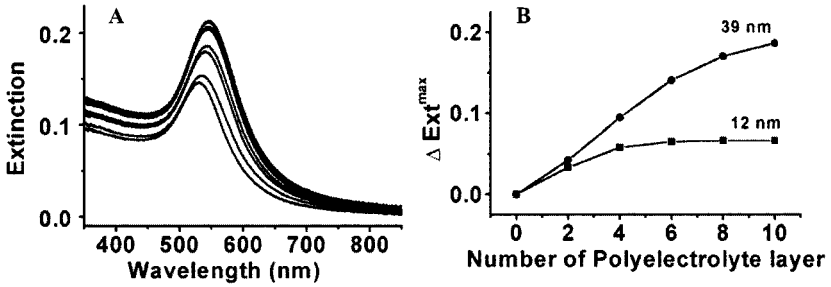

Fig. 6. A) Change in extinction spectrum of a 12 nm diameter gold nanoparticle monolayer due to layer-by-layer deposition of polyelctrolytes. B) Peak extinction as a function of the number of deposited polyelectrolyte layers for 12 nm and 39 nm diameter gold nanoparticles immobilized onto an amine-functionalized glass surface.

exciting opportunity to undertake a systematic experimental investigation of the effect of the composition, size and shape of nanoparticles upon their performance as nanoSPR sensors.

A second and important property of nanoSPR sensors, which has implications for the actual performance of the sensor in quantifying receptor-analyte interactions, is the sensing distance of the sensor. The sensing distance is the distance from the surface of the nanostructure extending into the bulk solution within which a change in refractive index can be detected. We used layer-by-layer deposition to sequentially deposit polyelectrolyte layers of opposite charge on immobilized gold nanoparticles with a diameter of 12 nm and 39 nm to systematically vary the thickness of the overlayer [45,46]. Positively charged poly(allylamine) hydrochloride (PAH; MW = 70,000 Da) and negatively charged polystyrene sulfonate (PSS; MW = 70,000 Da) were used for layer-by-layer deposition. Ten polyelectrolyte layers were deposited on the surface and the extinction spectrum of the immobilized gold nanoparticles was measured after each step.

Typical results for a nanoSPR chip fabricated from 12 nm diameter gold particles are shown in Fig. 6A. The ΔExt^{max} for 12 nm and 39 nm diameter gold particles is plotted for layers 0, 2, 4, 6, 8, 10 (Fig. 6B). There are two important observations that are relevant to the performance of these immobilized nanoparticles as nanoSPR transducers. First, the magnitude of extinction change (ΔExt^{max}) in response to polyelectrolyte deposition increases with particle size and second, the ΔExt^{max} saturates at a much smaller number of layers for smaller nanoparticles, indicating that smaller particles have a smaller sensing distance compared to larger nanoparticles.

Receptor-Analyte Detection by NanoSPR

We selected the streptavidin-biotin binding interaction for proof-of-concept studies of the immobilized nanoSPR sensor [9] because the wide use of this model system for validation of other biosensors enables comparison of the nanoSPR biosensor with other platforms under development [10,47–49]. A monolayer of ~39 nm spherical gold nanoparticles on glass was functionalized by formation of a SAM of 3-mercaptopropionic acid (MPA) to present terminal COOH groups at the surface of the gold nanoparticles. The COOH groups were then activated with a 1:1 mixture of 1-ethyl-3-(dimethylamino)propyl carbodiimide (EDAC) and pentafluorophenol (PFP) in ethanol and then reacted with an amine-terminated biotin derivative (biotin-amine) to covalently tether the biotin to the gold surface. The biotin-functionalized nanoSPR chip was subsequently incubated with 5.0 μg/mL of streptavidin for 3 hr, and the extinction spectrum of the nanoparticle monolayer was measured in a conventional UV-visible spectrophotometer. A shift in λ^{max} and an increase in Ext^{max} were observed for each functionalization step (Fig. 7), which is consistent with an increase in

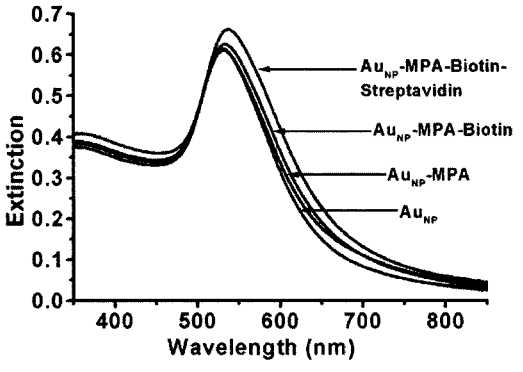

Fig. 7. Change in the extinction spectrum of immobilized gold nanoparticles (~39 nm diameter) on glass after each step in functionalization. Legend: Au_{NP}: gold nanoparticle on glass; Au_{NP}–MPA; Au_{NP} with a SAM of MPA; Au_{NP}–MPA-Biotin: Au_{NP}–MPA with covalently bound biotin at the surface; and Au_{NP}–MPA-Biotin-streptavidin: Au_{NP}–MPA-Biotin after incubation with 5.0 μg/mL of streptavidin.

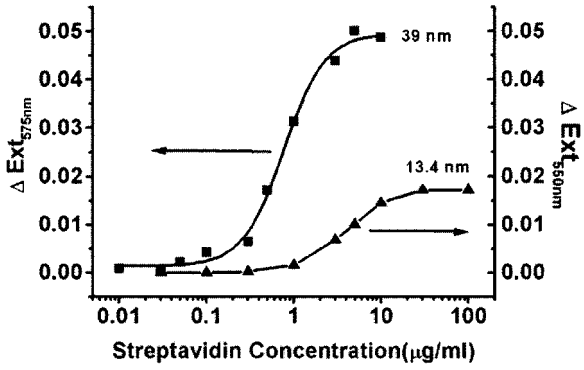

Fig. 8. Extinction change at 575 nm for immobilized 39 nm (squares) diameter and at 550 nm for 13.4 nm diameter (triangles) spherical gold nanoparticles that were functionalized with biotin as a function of streptavidin concentration.

the local refractive index. These results demonstrate that a chemisorbed monolayer of gold nanoparticles on glass can be used to transduce ligand-receptor binding at a surface into an extinction change with a sensitivity that is useful for biosensor applications.

We further investigated the concentration-dependent extinction change to determine the dynamic range and sensitivity that can be achieved for streptavidin-biotin binding using this sensor. Biotin functionalized sensor chips fabricated from spherical gold nanoparticles with a diameter of ∼39 nm were incubated with streptavidin as a function of solution concentrations ranging from 0.01 μg/mL to 10 μg/mL, and the extinction change at 575 nm was measured as a function of time. A calibration plot of the absorbance change at 575 nm, as a function of streptavidin concentration for immobilized 39 nm gold particles is shown in Fig. 8 along with the calibration plot for a nanoSPR sensor fabricated from 13.4 nm diameter gold nanoparticles and reported earlier by us [9]. These results clearly show that the nanoSPR sensor fabricated using 39 nm gold nanoparticles has a much higher sensitivity for the streptavidin-biotin interaction. This finding is also consistent with the higher sensitivity to the local refractive index and larger sensing distance of the 39 nm particles as compared to a nanoSPR sensor fabricated from 13.4 nm diameter gold nanoparticles.

The strong scattering properties of noble metal nanoparticles is also potentially of interest in the development of nanoparticle biosensors. This is because the extinction of noble metal nanoparticles has contributions from both absorbance and scattering. The extinction of small nanoparticles is dominated by their absorbance but scattering becomes the major component with an increase in particle size. For example, for 20 nm gold particles, the ratio of their scattering to absorbance cross section is 0.014, but this ratio increases two-hundred fold for 100 nm diameter gold particles [11,12]. Gold and silver nanoparticles are also much stronger light scatterers due to their plasmon resonance, as compared to particles that do not exhibit plasmon resonance; a 30 nm silver particle scatters light ∼2000 times more strongly than a polystyrene particle of the same size. Due to their large scattering cross-section, single nanoparticles of gold or silver that are adsorbed on to an optically transparent surface can be easily visualized by dark field optical microscopy, despite being smaller than the diffraction limit of visible light.

The change in refractive index of the surrounding medium also changes the spectrum of the scattered light-a property that has been used to design a single nanoparticle optical sensor. Schultz and colleagues have demonstrated that single spherical silver nanoparticles (diameter 40–90 nm, peak resonance wavelength ∼400–480 nm) have an average sensitivity of 160 nm/RIU in a single particle detection mode, and that the sensitivity of silver nanoprisms (longest dimension 55–120 nm; peak resonance wavelength ∼600–700 nm) is 350 nm/RIU [50]. The advantage of single particle sensing includes the reduction in sample volume and the potential for large scale multiplexing, although the requirement for integrating single particle nanoparticle sensor with sample dispensing and detecting unit are technological challenges that need to be addressed.

DIRECT SURFACE FABRICATION OF NANOSTRUCTURES FOR NANOSPR

There are number of other methods to fabricate nanostructures suitable for nanoSPR on surfaces that do not involve the chemical synthesis of noble metal nanoparticles and their immobilization on a surface. The two most common methods high-resolution lithography and nanosphere lithography are briefly reviewed in this section.

Fabrication of NanoSPR Sensors by Sub-Micron Lithography

Optical lithography is the key technological driving force in the semiconductor industry. Over past three decades, the feature size of semiconductor devices fabricated by optical lithography has shrunk from 15 μm in the first generation of integrated chips, to features with dimensions of ∼180 nm in current devices [51]. The ensemble of fabrication techniques that are centered around optical

lithography can also be easily adapted to create supported arrays of gold and silver nanostructures with sub-micron dimensions for nanoSPR.

Conventional optical lithography cannot, however, be used to fabricate features with sizes of a few tens of nanometers. This is because the resolution limit in optical lithography is defined by Rayleigh's equation $R = k_1\lambda/NA$ where λ is the wavelength of the light, NA is the numerical aperture of the optical system and k_1 is a constant that depends on the experimental setup and varies from 0.4 to 1.0 [52]. The practical resolution is usually close to the wavelength of the light used for photolithography and is currently around 180 nm for ultraviolet sources.

Several new high resolution lithographic techniques capable of fabricating sub-100 nm size features are consequently under development such as extreme ultraviolet lithography (EUV), X-ray lithography, and electron beam and ion beam lithography [51,52]. EUV and X-ray lithography use wavelengths of 11–13 nm and 1 nm respectively, and therefore allow the fabrication of features with lateral dimensions of several tens of nanometers. Although these techniques enable very small nanoscale features to be fabricated, they are technologically challenging to implement and are also extremely expensive, so that access to these fabrication methodologies is currently limited.

E-beam lithography (EBL) is an alternative approach for nanofabrication, which uses magnetic lenses to focus an electron beam to a submicron spot size. The focused e-beam is rastered to directly write a desired pattern onto a resist-coated substrate. In a recent use of EBL for nanoSPR, an array of nanostructures fabricated by EBL, was used to study the effect of the interparticle separation on plasmon coupling [53,54]. These studies showed that λ^{max} of the nanostructure red-shifts as a result of interparticle interactions, and that the interaction decays exponentially with increasing interparticle separation and becomes negligible when the distance between the particles exceeds the particle size by a factor of 2.5 [53].

EBL was also recently used as a fabrication technique to demonstrate that the interparticle coupling of plasmons can be used to transport electromagnetic energy below the diffraction limit [55]. An array of rod shaped silver nanoparticles with dimensions of 90 nm $\times$ 30 nm $\times$ 30 nm separated by 50 nm were fabricated by EBL, and a near field-scanning optical microscope (NSOM) was used to excite surface plasmons in a single silver nanoparticle in this array. The excited plasmons were shown to couple into neighboring particles, resulting in propagation of the incident light along the nanoparticle array. A fluorescent particle, with an excitation wavelength that overlapped the surface plasmon wavelength, could then be excited up to 500 nm away from the NSOM source by the propagated surface plasmons.

The advantages of creating nanostructures using EBL include exact control over the shape and size of the features and the ability to control the interfeature separation. EBL is a very useful fabrication technique to prototype nanostructures for nanoSPR and two recent studies illustrate the utility of this fabrication methodology for fundamental research in nanoSPR. The primary limitation of EBL for the fabrication of noble metal nanostructures on a surface is that EBL is a serial processing method, and can therefore only be used to create nanostructures over a small area. This precludes its use at this time for the low-cost, high-volume fabrication of supported metal nanostructures for nanoSPR.

Recently, several new low cost, high-resolution and high-throughput fabrication techniques for generating nanostructures have been developed such as nanoimprint lithography [56–58], soft lithography [59–61], and dip-pen nanolithography [62–65]. The relative advantages and limitations of these technologies for fabrication of noble metal structures on the surface for design of nanoSPR biosensors remains a relatively unexplored area of investigation at this time.

Direct Deposition of Metals Nanoislands

Rubinstein and colleagues have demonstrated that nanoislands of gold can be directly fabricated onto glass simply by controlling the deposition conditions [66]. They showed that ultrathin gold films (thickness of $<$10 nm) evaporated on a transparent substrate typically form nanoscale island-like structures whose size and interfeature separation can be controlled by changing the evaporation parameters. The optical spectra of these metal nanoislands show a plasmon resonance peak at $\sim$600 nm. They also showed that the adsorption of different molecular species on these thin gold nanoislands causes a red-shift in the plasmon resonance wavelength as well as an increase in the absorbance intensity, parameters, that were used to follow the kinetics of adsorption of a small cyclic disulfide. A similar strategy was also used to detect the hybridization of an oligonucleotide to its complementary strand that was immobilized on the gold nanoislands [67]. They also observed that enhanced sensitivity from DNA hybridization was obtained when the probe oligonucleotide was labeled with gold nanoparticles, probably due to surface plasmon coupling between the gold island on the surface and the gold nanoparticles attached to the probe oligonucleotide. The most attractive feature of this fabrication method is its simplicity in that it does not require sophisticated lithography or masking techniques, and a minimal number of

processing steps. On the other hand, this method has significant limitations in the lack of precise control over the nanoisland shape, the interfeature separation, and lack of long-range order.

NanoSPR Fabricated by Nanosphere Lithography

Nanosphere lithography (NSL), pioneered by Van Duyne and colleagues, is the third fabrication method that has been used to create nanostructures directly on optically transparent substrates. NSL involves coating a glass substrate with a suspension of polystyrene nanospheres where they self assemble in a hexagonal closed packed array. The substrate is then mounted in a vacuum chamber and silver or gold is deposited through the mask created by the close-packed polystyrene particles [68–70]. The substrate is then removed from the chamber, and the polystyrene particles are removed leaving behind truncated tetrahedral nanostructures of the deposited metal on the surface. The size of the nanostructures and their spacing can be changed by changing the size of polystyrene nanospheres that are used as the physical mask and by varying the amount of deposited metal.

Truncated tetrahedral nanostructures of silver created using NSL (Fig. 9) exhibit a plasmon resonance band that is tunable from 400 to 6000 nm simply by changing the size and shape of the nanostructures [68]. The optical properties of tetrahedral silver nanostructures have also been shown to be extremely sensitive to the refractive index of their surrounding medium, with a maximum peak resonance wavelength shift of $\sim$200 nm/RIU, so that these nanostructures are capable of optically transducing small changes in refractive index that accompany the receptor ligand binding at the nanoparticle surface. In a recent study, these supported silver nanostructures exhibited a limit of detection (LOD) of $<$1 pM for the streptavidin-biotin interaction [10]. Van Duyne and colleagues have also recently shown that these nanostructures can be used in the scattering mode for biomolecular detection [71].

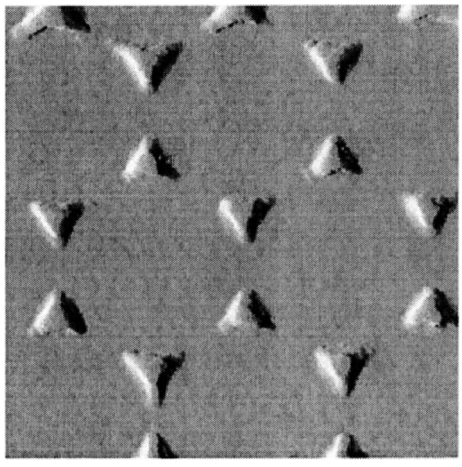

Fig. 9. Tapping mode AFM image of a silver nanoparticle array fabricated by nanosphere lithography on a glass substrate. Image area is 1 μm $\times$ 1 μm. Polystyrene sphere with a diameter of 400 nm were self-assembled on glass to create the mask for nanosphere lithography, and the height of the silver nanostructure is 50 nm. Reprinted with permission *J. Am. Chem. Soc.* 2001, **123**, 1471–1482. Copyright 2001 American Chemical Society.

The lower LOD obtained with silver nanostructures as compared to gold nanospheres is due to two reasons: first, silver nanoparticles have an intrinsically greater sensitivity in nanoSPR compared to gold for nanoparticles of the same size and shape. More importantly however, anisotropic nanostructures such as truncated tetrahedron are more sensitive than isotropic particles (e.g., spheres) to the refractive index of the surrounding medium. As noted in the previous section, a comparable sensitivity can be achieved in nanoSPR by sensors that are fabricated via self-assembly of chemically synthesized anisotropic particles. Although NSL is a useful method for fabrication of nanoSPR sensors, polystyrene colloids are difficult to assemble at high coverage over large areas without introducing significant defects, so that their use as disposable masks in NSL make this fabrication methodology rather expensive and impractical for high-volume fabrication of nanoSPR chips. Nevertheless, NSL remains a simple and useful method for the bench-top fabrication of supported metal nanostructures for research in nanoSPR.

FUTURE DIRECTIONS

Prospects

The future is bright for nanoscale photonics biosensors. We believe that the colorimetric changes of an ensemble of supported metal nanostructures in response to analyte binding is an exquisitely simple technology that will enable the development of low-cost, miniaturized and rugged optical sensors for the real-time, label-free optical detection of a wide variety of biomolecular interactions. These sensors are likely to be useful in diverse operating environments ranging from field-use, point-of-care clinical diagnostics and sensors to bioanalytical devices for laboratory use. In comparison with many other approaches for the fabrication of nanoscale sensors, nanoSPR is unique in terms of its simple fabrication as well as detection using conventional light transmission or scattering through an ensemble of supported metal nanostructures.

In the near term, the extension of single channel nanoSPR to multiplexed sensors is an immediate technological challenge to be met. There are at least two different approaches that can be taken to fabricate multiplexed nanoSPR sensors that can integrate nanoSPR with commercially available instrumentation to create high-throughput, low cost biosensors that are compatible with current assay formats. In the first approach, receptor-functionalized nanoparticles can be assembled within conventional 96/384/1536 well plates and their color change in response to biomolecular binding can be measured on a multiwell plate reader, which takes advantage of the ubiquity of multiwell absorbance plate readers. In a second approach, functionalized nanoparticles can also be spotted onto functionalized glass slides by a robotic arrayer and the array can be interrogated by a CCD camera.

Another approach to multiplexing nanoSPR sensors is to functionalize metallic nanoparticles that have unique optical signatures with different receptors [25]. We envision that with advances in nanoparticle synthesis, it will be possible to synthesize a diverse library of noble metal nanoparticles such that each type of nanoparticle in the library will have a unique optical response to biomolecular binding. This approach will enable large scale multiplexing of nanoSPR based on the unique optical response of each member of that library.

Finally, the ability to optically image a single metal nanoparticle due to its extremely high scattering cross section opens up new vistas in the design of single particle nanoSPR biosensors. One potential design that can be envisioned is that of individual nanoparticles that are functionalized with different receptors incorporated into a nano/micro fluidics channel. The integration of single nanoSPR in lab-on–a-chip bioanalytical devices [72–76] will enable the ultrasensitive detection of a large number of analytes in a single device.

Challenges

The precise control over the size and shape of noble metal nanostructures is essential to engineer the optical properties of nanoSPR sensors as well as to ensure the long-term reproducibility of nanoSPR assays. Although the synthesis of metal nanoparticles has a long history [77], the chemical synthesis of metal nanoparticles remains, to this date, a curious admixture of art and science. At this time, limited methods are available even to reproducibly synthesize the simplest nanostructures such as monodisperse spherical gold and silver nanoparticles. The syntheses of anisotropic particles, cubes and prisms, have been recently reported [24,26,27,78] and efforts are underway to understand the mechanism behind the shape selectivity of these syntheses as well as to control the heterogeneity in the size and shape of these nanostructures. In parallel, progress in unconventional "top down" nanolithography techniques and "bottom up" nanoassembly approaches to fabrication of nanoSPR sensors will also enable inexpensive, large-scale fabrication of metal nanostructures directly on a substrate that are suitable for nanoSPR.

Finally, the relative lack of mechanistic understanding of the principles that govern nanoparticle formation also remains a critical hurdle that must be overcome to accelerate the development of nanoSPR biosensors. Although significant progress has been made in developing a theoretical understanding of the optical properties of nanoparticles as a function of their size, shape and composition, a systematic investigation of the optical properties of nanostructures with the specific goal of optimizing their performance as nanoSPR sensors has been lacking. We believe that a tightly coupled theoretical and experimental approach is required to quantify the effect of the composition and structure of nanoparticles on their performance as nanoSPR sensors. These studies will ultimately, we believe, lead to the development of quantitative models that will allow *ab initio* design of nanoSPR biosensors, a goal that remains elusive at this time.

REFERENCES

1. J. Fritz, M. K. Baller, H. P. Lang, H. Rothuizen, P. Vettiger, E. Meyer, H. J. Guntherodt, C. Gerber, and J. K. Gimzewski (2000). Translating biomolecular recognition into nanomechanics. *Science* **288**(5464), 316–318.
2. G. H. Wu, R. H. Datar, K. M. Hansen, T. Thundat, R. J. Cote, and A. Majumdar (2001). Bioassay of prostate-specific antigen (PSA) using microcantilevers. *Nat. Biotechnol.* **19**(9), 856–860.
3. R. R. Shah and N. L. Abbott (2001). Principles for measurement of chemical exposure based on recognition-driven anchoring transitions in liquid crystals. *Science* **293**(5533), 1296–1299.
4. K. B. Lee, S. J. Park, C. A. Mirkin, J. C. Smith, and M. Mrksich (2002). Protein nanoarrays generated by dip-pen nanolithography. *Science* **295**(5560), 1702–1705.
5. L. R. Hirsch, J. B. Jackson, A. Lee, N. J. Halas, and J. L. West (2003). A whole blood immunoassay using gold nanoshells. *Anal. Chem.* **75**(10), 2377–2381.
6. T. A. Taton, C. A. Mirkin, and R. L. Letsinger (2000). Scanometric DNA array detection with nanoparticle probes. *Science* **289**(5485), 1757–1760.
7. J. J. Storhoff, R. Elghanian, R. C. Mucic, C. A. Mirkin, and R. L. Letsinger (1998). One-pot colorimetric differentiation of polynucleotides with single base imperfections using gold nanoparticle probes. *J. Am. Chem. Soc.* **120**(9), 1959–1964.
8. R. Elghanian, J. J. Storhoff, R. C. Mucic, R. L. Letsinger, and C. A. Mirkin (1997). Selective colorimetric detection of polynucleotides based on the distance-dependent optical properties of gold nanoparticles. *Science* **277**(5329), 1078–1087.
9. N. Nath and A. Chilkoti (2002). A colorimetric gold nanoparticle sensor to interrogate biomolecular interactions in real time on a surface. *Anal. Chem.* **74**(3), 504–509.

10. A. J. Haes and R. P. Van Duyne (2002). A nanoscale optical biosensor: sensitivity and selectivity of an approach based on the localized surface plasmon resonance spectroscopy of triangular silver nanoparticles. *J. Am. Chem. Soc.* **124**(35), 10596–10604.
11. J. Yguerabide and E. E. Yguerabide (1998). Light-scattering submicroscopic particles as highly fluorescent analogs and their use as tracer labels in clinical and biological applications—I. Theory. *Anal. Biochem.* **262**(2), 137–156.
12. J. Yguerabide and E. E. Yguerabide (1998). Light-scattering submicroscopic particles as highly fluorescent analogs and their use as tracer labels in clinical and biological applications—II. Experimental characterization. *Anal. Biochem.* **262**(2), 157–176.
13. U. Kreibig and M. Vollmer (1995). *Optical Properties of Metal Clusters*, Springer-Verlag, Berlin.
14. S. Link and M. A. El-Sayed (2000). Shape and size dependence of radiative, non-radiative and photothermal properties of gold nanocrystals. *Int. Rev. Phys. Chem.* **19**(3), 409–453.
15. E. D. Palik. (1984). *Handbook of Optical Constants of Solids*, Academic Press, Boston.
16. A. A. Lazarides and G. C. Schatz (2000). DNA-linked metal nanosphere materials: Structural basis for the optical properties. *J. Phys. Chem. B* **104**(3), 460–467.
17. J. Turkevich (1985). Colloidal Gold. Part 1. *Gold Bulletin* **18**(3), 86–91.
18. D. V. Goia and E. Matijevic (1998). Preparation of monodispersed metal particles. *New J. Chem.* **22**(11), 1203–1215.
19. D. V. Goia and E. Matijevic (1999). Tailoring the particle size of monodispersed colloidal gold. *Colloids Surf. A-Physicochem. Eng. Aspects* **146**(1–3), 139–152.
20. M. Brust, M. Walker, D. Bethell, D. J. Schiffrin, and R. Whyman (1994). Synthesis of thiol-derivatized gold nanoparticles in a 2-phase liquid-liquid system. *J. Chem. Soc., Chem. Commun.* (7), 801–802.
21. P. Y. Silvert, R. HerreraUrbina, N. Duvauchelle, V. Vijayakrishnan, and K. T. Elhsissen (1996). Preparation of colloidal silver dispersions by the polyol process .1. Synthesis and characterization. *J. Mater. Chem.* **6**(4), 573–577.
22. Y. Cao, R. Jin, and C. A. Mirkin (2001). DNA-modified core-shell Ag/Au nanoparticles. *J. Am. Chem. Soc.* **123**(32), 7961–7962.
23. D. A. Handley (1989). Methods for synthesis of colloidal gold. in M. A. Hayat (Ed.), *Colloidal Gold: Principles, Methods, and Applications* (Vol. 1) Academic Press, San Diego, CA, pp. 13–32.
24. C. J. Murphy and N. R. Jana (2002). Controlling the aspect ratio of inorganic nanorods and nanowires. *Adv. Mater.* **14**(1), 80–82.
25. S. R. Nicewarner-Pena, R. G. Freeman, B. D. Reiss, L. He, D. J. Pena, I. D. Walton, R. Cromer, C. D. Keating, and M. J. Natan (2001). Submicrometer metallic barcodes. *Science* **294**(5540), 137–141.
26. R. C. Jin, Y. W. Cao, C. A. Mirkin, K. L. Kelly, G. C. Schatz, and J. G. Zheng (2001). Photoinduced conversion of silver nanospheres to nanoprisms. *Science* **294**(5548), 1901–1903.
27. Y. Sun and Y. Xia (2002). Shape-controlled synthesis of gold and silver nanoparticles. *Science* **298**(5601), 2176–2179.
28. C. J. Johnson, E. Dujardin, S. A. Davis, C. J. Murphy, and S. Mann (2002). Growth and form of gold nanorods prepared by seed-mediated, surfactant-directed synthesis. *J. Mater. Chem.* **12**(6), 1765–1770.
29. N. R. Jana, L. Gearheart, and C. J. Murphy (2001). Seed-mediated growth approach for shape-controlled synthesis of spheroidal and rod-like gold nanoparticles using a surfactant template. *Adv. Mater.* **13**(18), 1389–1393.
30. S. J. Oldenburg, R. D. Averitt, S. L. Westcott, and N. J. Halas (1998). Nanoengineering of optical resonances. *Chem. Phys. Lett.* **288**(2–4), 243–247.
31. Y. G. Sun and Y. N. Xia (2003). Gold and silver nanoparticles: A class of chromophores with colors tunable in the range from 400 to 750 nm. *Analyst* **128**(6), 686–691.
32. P. Englebienne (1998). Use of colloidal gold surface plasmon resonance peak shift to infer affinity constants from the interactions between protein antigens and antibodies specific for single or multiple epitopes. *Analyst* **123**(7), 1599–1603.
33. P. Englebienne, A. Van Hoonacker, and J. Valsamis (2000). Rapid homogeneous immunoassay for human ferritin in the cobas mira using colloidal gold as the reporter reagent. *Clin. Chem.* **46**(12), 2000–2003.
34. R. G. Freeman, K. C. Grabar, K. J. Allison, R. M. Bright, J. A. Davis, A. P. Guthrie, M. B. Hommer, M. A. Jackson, P. C. Smith, D. G. Walter, and M. J. Natan (1995). Self-assembled metal colloid monolayers—an Approach to SERS substrates. *Science* **267**(5204), 1629–1632.
35. K. C. Grabar, R. G. Freeman, M. B. Hommer, and M. J. Natan (1995). Preparation and characterization of Au colloid monolayers. *Anal. Chem.* **67**(4), 735–743.
36. T. Okamoto, I. Yamaguchi, and T. Kobayashi (2000). Local plasmon sensor with gold colloid monolayers deposited upon glass substrates. *Opt. Lett.* **25**(6), 372–374.
37. H. Nakamura and I. Karube (2003). Current research activity in biosensors. *Anal. Bioanal. Chem.* **377**(3), 446–468.
38. S. S. Iqbal, M. W. Mayo, J. G. Bruno, B. V. Bronk, C. A. Batt, and J. P. Chambers (2000). A review of molecular recognition technologies for detection of biological threat agents. *Biosens. Bioelectron.* **15**(11–12), 549–578.
39. B. M. Paddle (1996). Biosensors for chemical and biological agents of defence interest. *Biosens. Bioelectron.* **11**(11), 1079–1113.
40. P. VanDerVoort and E. F. Vansant (1996). Silylation of the silica surface a review. *J. Liq. Chromatogr. Relat. Technol.* **19**(17–18), 2723–2752.
41. M. D. Malinsky, K. L. Kelly, G. C. Schatz, and R. P. Van Duyne (2001). Chain length dependence and sensing capabilities of the localized surface plasmon resonance of silver nanoparticles chemically modified with alkanethiol self-assembled monolayers. *J. Am. Chem. Soc.* **123**(7), 1471–1482.
42. Y. G. Sun and Y. N. Xia (2002). Increased sensitivity of surface plasmon resonance of gold nanoshells compared to that of gold solid colloids in response to environmental changes. *Anal. Chem.* **74**(20), 5297–5305.
43. W. H. Yang, G. C. Schatz, and R. P. Vanduyne (1995). Discrete dipole approximation for calculating extinction and Raman intensities for small particles with arbitrary shapes. *J. Chem. Phys.* **103**(3), 869–875.
44. E. J. Zeman and G. C. Schatz (1987). An accurate electromagnetic theory study of surface enhancement factors for Ag, Au, Cu, Li, Na, Al, Ga, in, Zn, and Cd. *J. Phys. Chem.-Us* **91**(3), 634–643.
45. G. Decher (1997). Fuzzy nanoassemblies: Toward layered polymeric multicomposites. *Science* **277**(5330), 1232–1237.
46. J. Schmitt, P. Machtle, D. Eck, H. Mohwald, and C. A. Helm (1999). Preparation and optical properties of colloidal gold monolayers. *Langmuir* **15**(9), 3256–3266.
47. G. MacBeath and S. L. Schreiber (2000). Printing proteins as microarrays for high-throughput function determination. *Science* **289**(5485), 1760–1763.
48. L. Movileanu, S. Howorka, O. Braha, and H. Bayley (2000). Detecting protein analytes that modulate transmembrane movement of a polymer chain within a single protein pore. *Nat. Biotechnol.* **18**(10), 1091–1095.
49. Y. Cui, Q. Wei, H. Park, and C. M. Lieber (2001). Nanowire nanosensors for highly sensitive and selective detection of biological and chemical species. *Science* **293**(5533), 1289–1292.
50. J. J. Mock, D. R. Smith, and S. Schultz (2003). Local refractive index dependence of plasmon resonance spectra from individual nanoparticles. *NanoLett.* **3**(4), 485–491.
51. T. Ito and S. Okazaki (2000). Pushing the limits of lithography. *Nature* **406**(6799), 1027–1031.
52. Y. Chen and A. Pepin (2001). Nanofabrication: Conventional and nonconventional methods. *Electrophoresis* **22**(2), 187–207.
53. K. H. Su, Q. H. Wei, X. Zhang, J. J. Mock, D. R. Smith, and S. Schultz (2003). Interparticle coupling effects on plasmon resonances of nanogold particles. *Nano Lett.* **3**(8), 1087–1090.

54. W. Rechberger, A. Hohenau, A. Leitner, J. R. Krenn, B. Lamprecht, and F. R. Aussenegg (2003). Optical properties of two interacting gold nanoparticles. *Opt. Commun.* **220**(1–3), 137–141.
55. S. A. Maier, P. G. Kik, H. A. Atwater, S. Meltzer, E. Harel, B. E. Koel, and A. A. G. Requicha (2003). Local detection of electromagnetic energy transport below the diffraction limit in metal nanoparticle plasmon waveguides. *Nat. Mater.* **2**(4), 229–232.
56. C. M. S. Torres, S. Zankovych, J. Seekamp, A. P. Kam, C. C. Cedeno, T. Hoffmann, J. Ahopelto, F. Reuther, K. Pfeiffer, G. Bleidiessel, G. Gruetzner, M. V. Maximov, and B. Heidari (2003). Nanoimprint lithography: An alternative nanofabrication approach. *Mater. Sci. Eng. C, Biomimetic Supramol. Syst.* **23**(1–2), 23–31.
57. S. Zankovych, T. Hoffmann, J. Seekamp, J. U. Bruch, and C. M. S. Torres (2001). Nanoimprint lithography: Challenges and prospects. *Nanotechnology* **12**(2), 91–95.
58. S. Y. Chou (2001). Nanoimprint lithography and lithographically induced self-assembly. *MRS Bull.* **26**(7), 512–517.
59. Y. N. Xia and G. M. Whitesides (1998). Soft lithography. *Angew. Chem., Int. Ed.* **37**(5), 551–575.
60. Y. N. Xia and G. M. Whitesides (1998). Soft lithography. *Annu. Rev. Mater. Sci.* **28**, 153–184.
61. Y. Xia, J. A. Rogers, K. E. Paul, and G. M. Whitesides (1999). Unconventional methods for fabricating and patterning nanostructures. *Chem. Rev.* **99**(7), 1823–1848.
62. R. D. Piner, J. Zhu, F. Xu, S. H. Hong, and C. A. Mirkin (1999). "Dip-pen" nanolithography. *Science* **283**(5402), 661–663.
63. C. A. Mirkin, S. H. Hong, and L. Demers (2001). Dip-pen nanolithography: Controlling surface architecture on the sub-100 nanometer length scale. *Chem. Phys. Chem.* **2**(1), 37–39.
64. S. H. Hong, J. Zhu, and C. A. Mirkin (1999). Multiple ink nanolithography: Toward a multiple-pen nano-plotter. *Science* **286**(5439), 523–525.
65. S. H. Hang and C. A. Mirkin (2000). A nanoplotter with both parallel and serial writing capabilities. *Science* **288**(5472), 1808–1811.
66. G. Kalyuzhny, M. A. Schneeweiss, A. Shanzer, A. Vaskevich, and I. Rubinstein (2001). Differential plasmon spectroscopy as a tool for monitoring molecular binding to ultrathin gold films. *J. Am. Chem. Soc.* **123**(13), 3177–3178.
67. E. Hutter and M. P. Pileni (2003). Detection of DNA hybridization by gold nanoparticle enhanced transmission surface plasmon resonance spectroscopy. *J. Phys. Chem. B* **107**(27), 6497–6499.
68. T. R. Jensen, M. D. Malinsky, C. L. Haynes, and R. P. Van Duyne (2000). Nanosphere lithography: Tunable localized surface plasmon resonance spectra of silver nanoparticles. *J. Phys. Chem. B* **104**(45), 10549–10556.
69. T. R. Jensen, M. L. Duval, K. L. Kelly, A. A. Lazarides, G. C. Schatz, and R. P. Van Duyne (1999). Nanosphere lithography: Effect of the external dielectric medium on the surface plasmon resonance spectrum of a periodic array of sliver nanoparticles. *J. Phys. Chem. B* **103**(45), 9846–9853.
70. W. Frey, C. K. Woods, and A. Chilkoti (2000). Ultraflat nanosphere lithography: A new method to fabricate flat nanostructures. *Adv. Mater.* **12**(20), 1515–1519.
71. A. D. McFarland and R. P. Van Duyne (2003). Single silver nanoparticles as real-time optical sensors with zeptomole sensitivity. *NanoLett.* **3**(8), 1057–1062.
72. C. Hansen and S. R. Quake (2003). Microfluidics in structural biology: smaller, faster . . . better. *Curr. Opin. Struct. Biol.* **13**(5), 538–544.
73. B. H. Weigl, R. L. Bardell, and C. R. Cabrera (2003). Lab-on-a-chip for drug development. *Adv. Drug Deliv. Rev.* **55**(3), 349–377.
74. T. H. Schulte, R. L. Bardell, and B. H. Weigl (2002). Microfluidic technologies in clinical diagnostics. *Clin. Chim. Acta* **321**(1–2), 1–10.
75. D. Figeys (2002). Adapting arrays and lab-on-a-chip technology for proteomics. *Proteomics* **2**(4), 373–382.
76. L. Mere, T. Bennett, P. Coassin, P. England, B. Hamman, T. Rink, S. Zimmerman, and P. Negulescu (1999). Miniaturized FRET assays and microfluidics: Key components for ultra-high-throughput screening. *Drug Discov. Today* **4**(8), 363–369.
77. M. Faraday (1857). Experimental relations of gold (and other metals) to light. *Philos. Trans. R. Soc. Lond.* **147**, 145–181.
78. R. C. Jin, Y. C. Cao, E. C. Hao, G. S. Metraux, G. C. Schatz, and C. A. Mirkin (2003). Controlling anisotropic nanoparticle growth through plasmon excitation. *Nature* **425**(6957), 487–490.